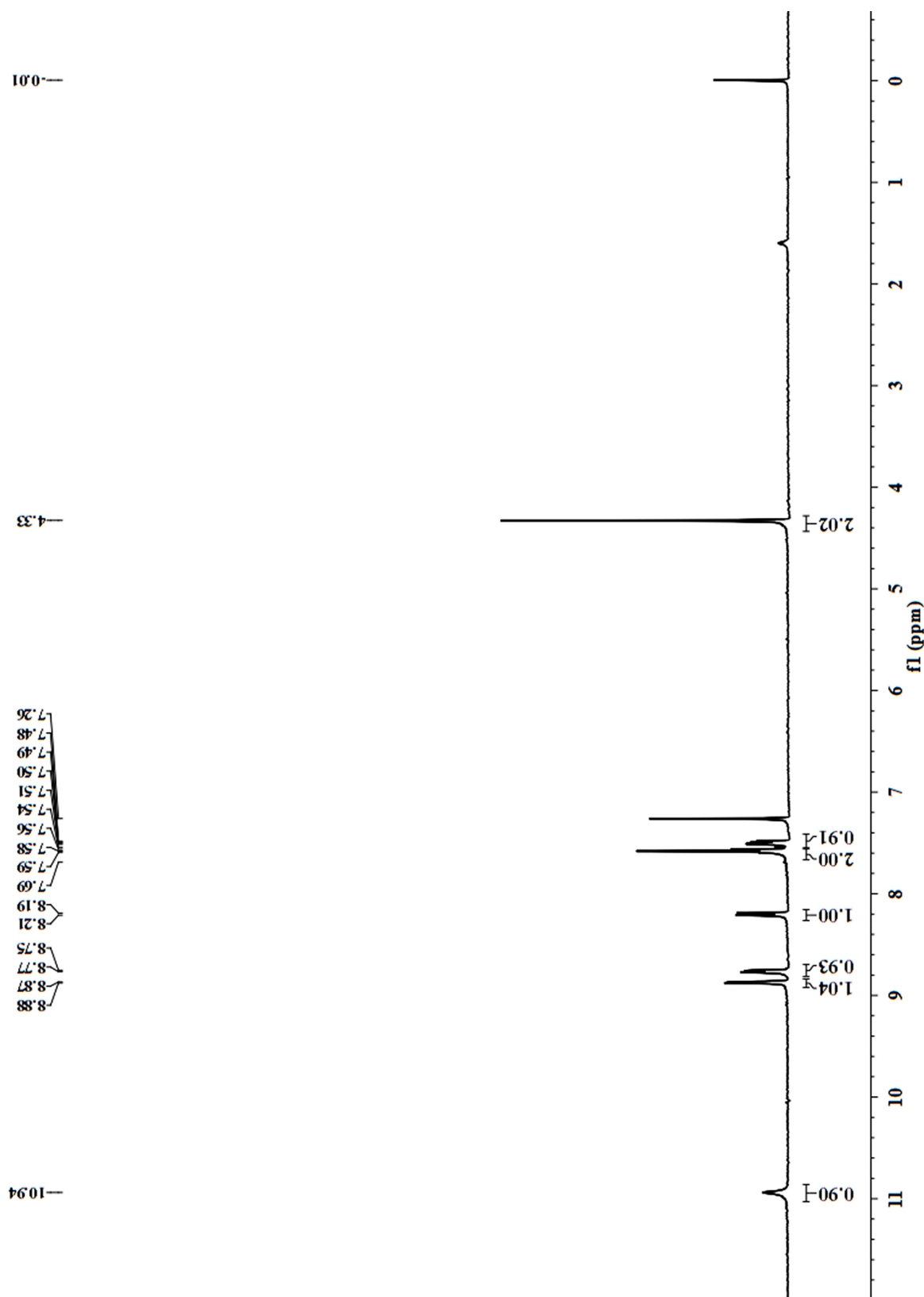
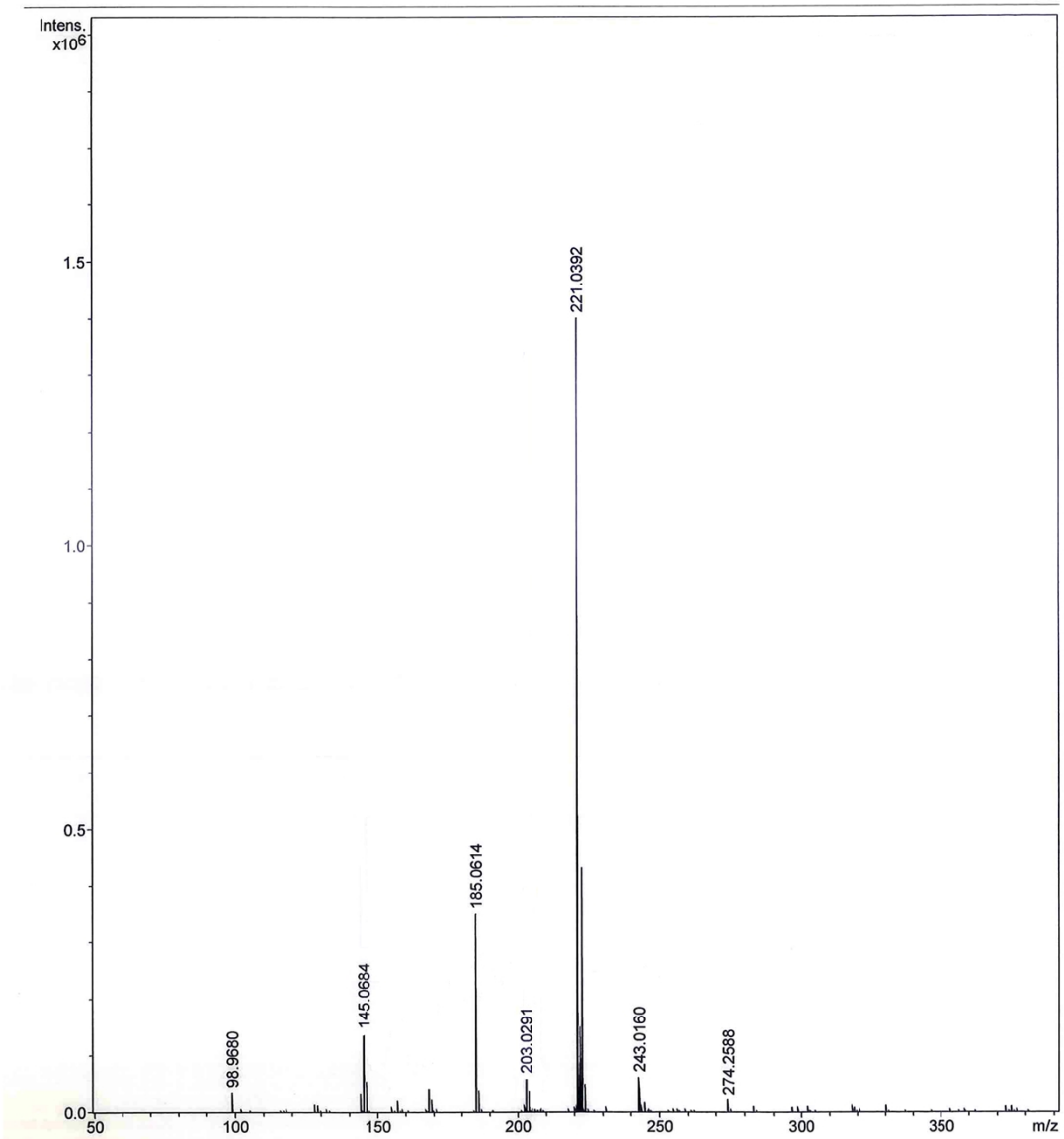


**Supplementary Material**



**Fig. S1**  $^1\text{H}$  NMR ( $\text{CDCl}_3$ , 400 MHz) spectrum of AQ-Cl.



**Fig. S2** ESI-MS spectrum of AQ-Cl.

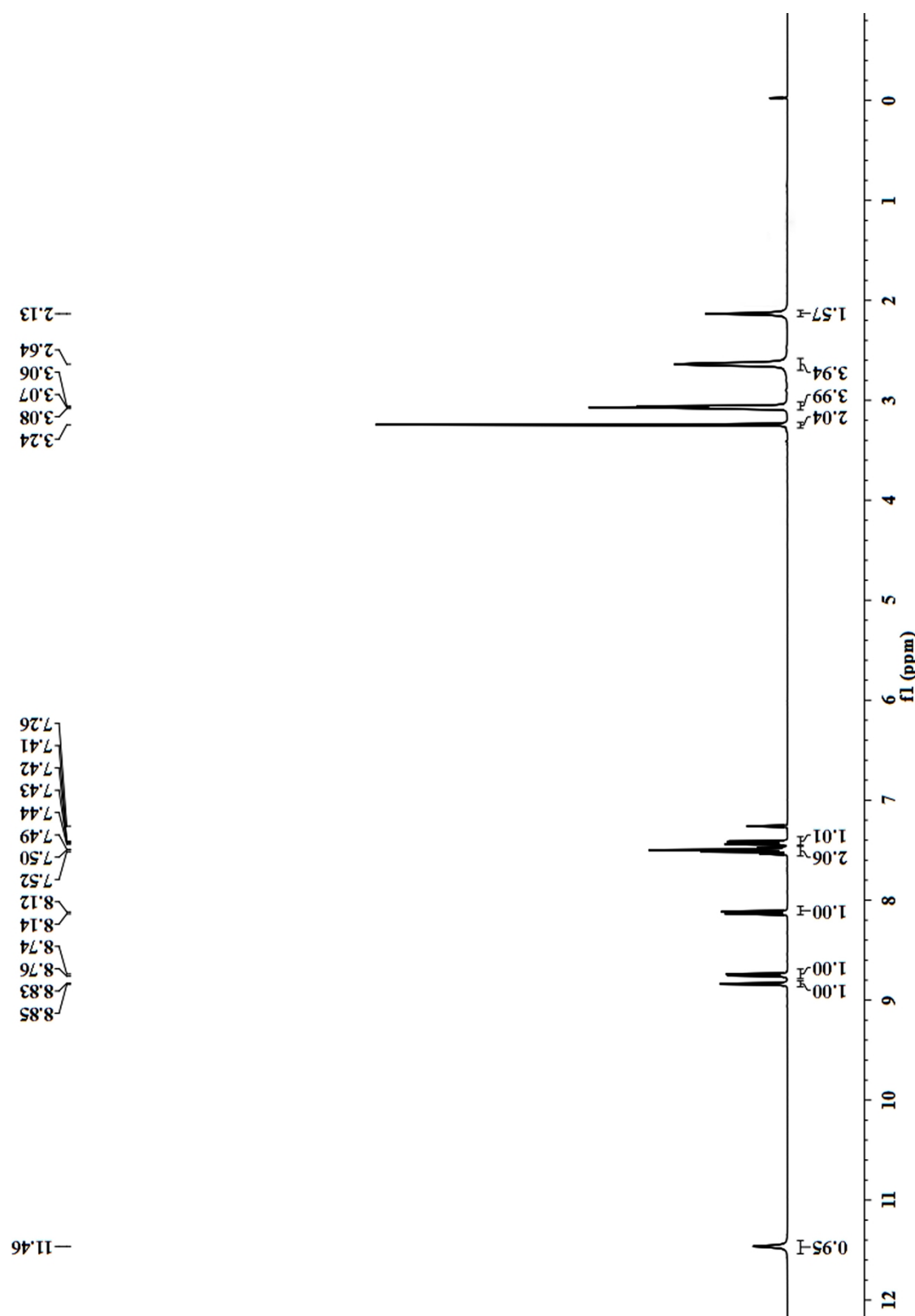


**Fig. S3**  $^1\text{H}$  NMR ( $\text{CDCl}_3$ , 400 MHz) spectrum of AQ-N.

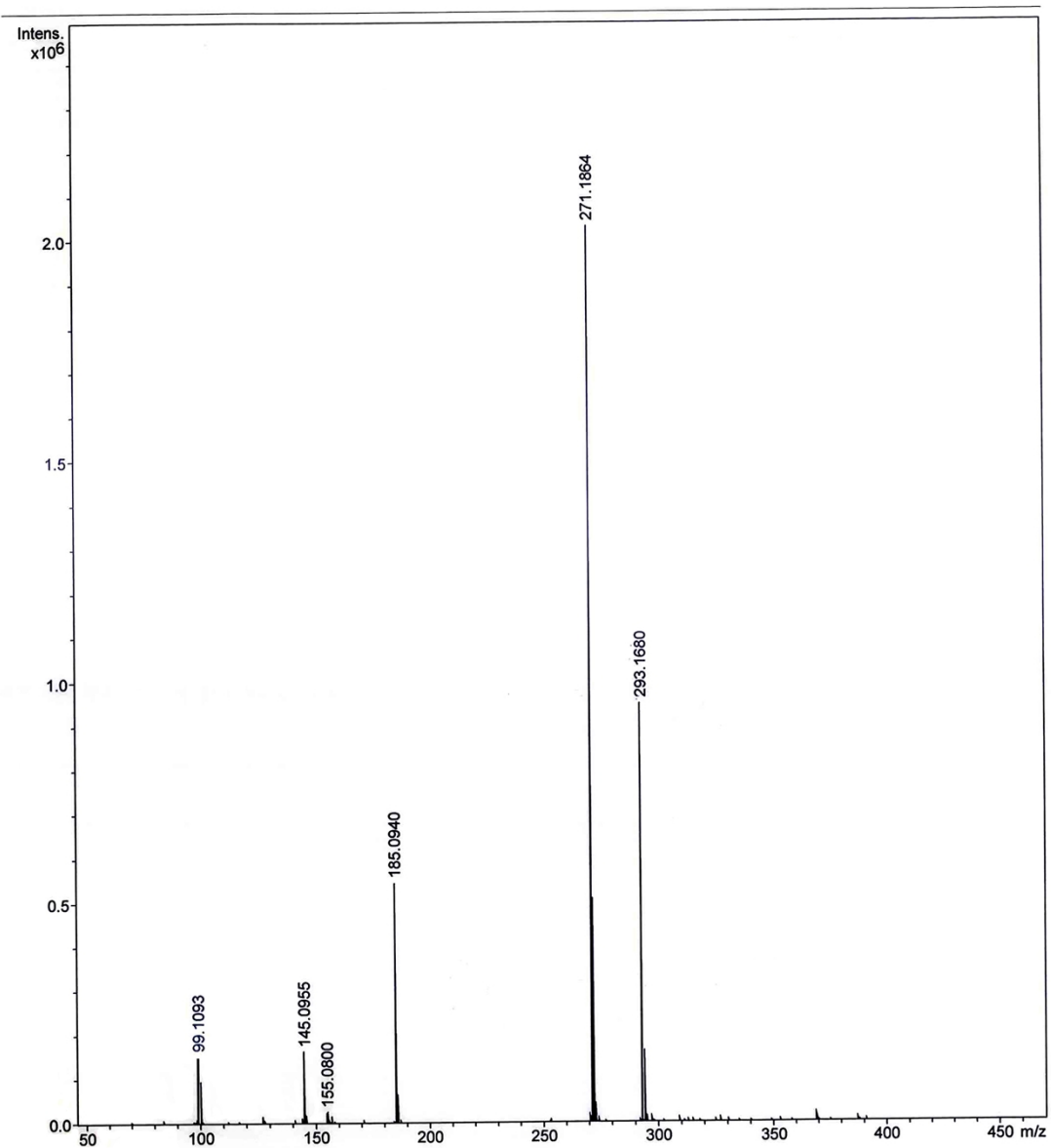


**Fig. S4** ESI-MS spectrum of AQ-N.

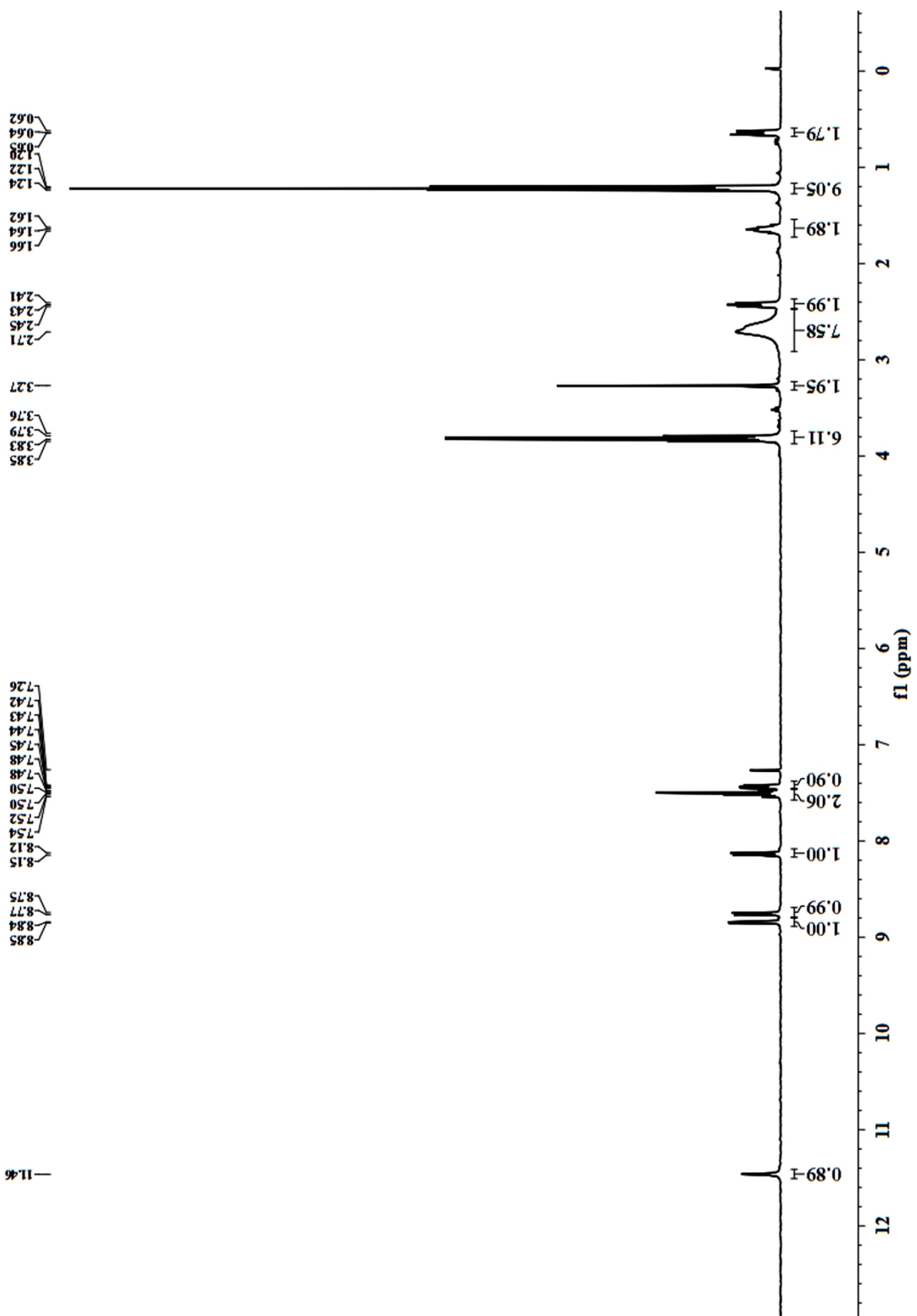


**Fig. S5**  $^1\text{H}$  NMR ( $\text{CDCl}_3$ , 400 MHz) spectrum of AQ-Si.

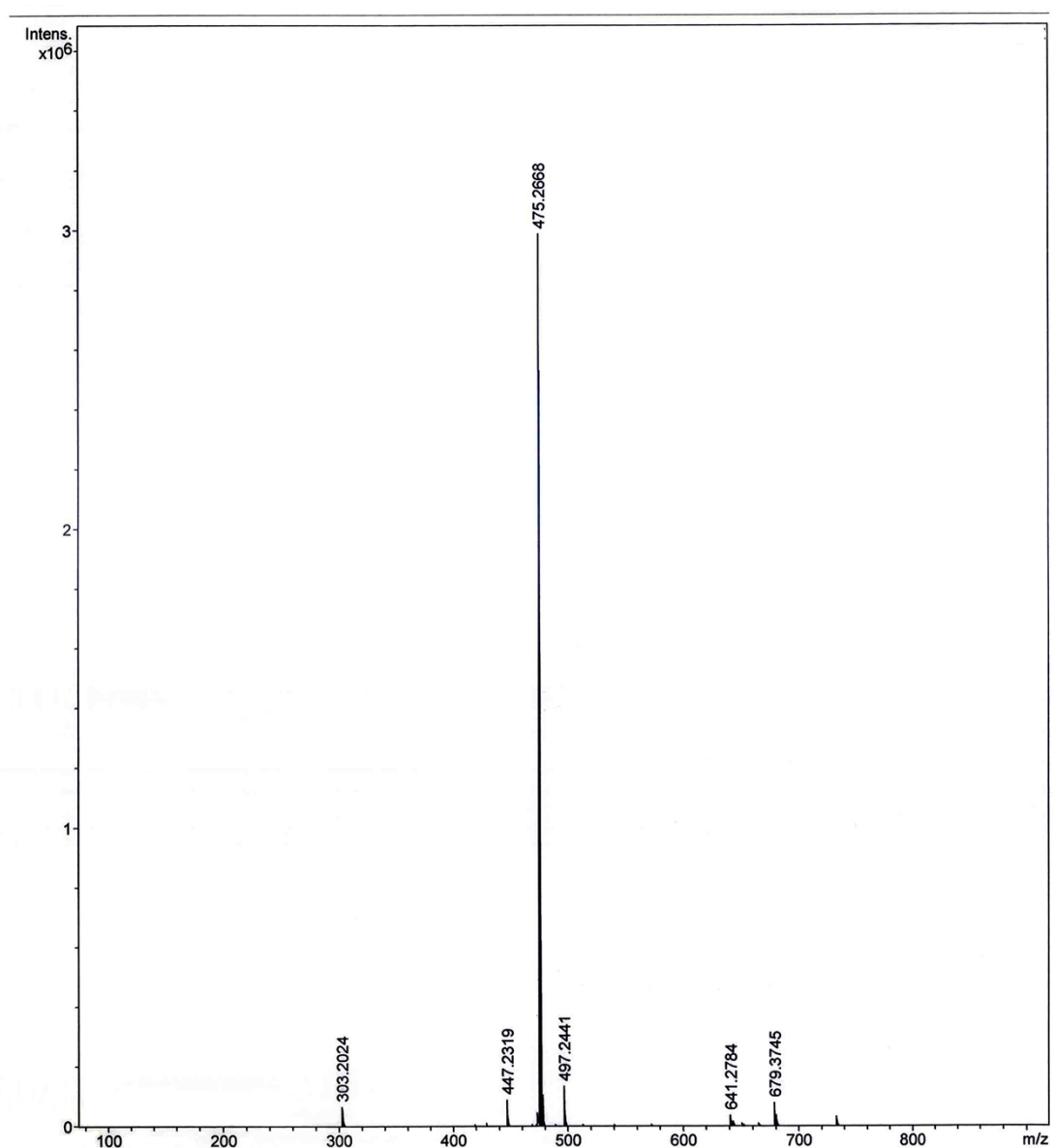


**Fig. S6** ESI-MS spectrum of AQ-Si.

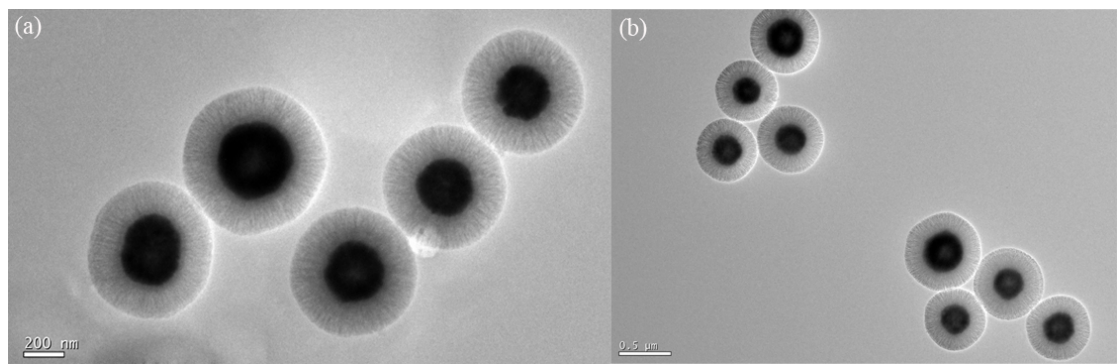


**Fig. S7.** Transmission electron microscopy images of **AQ-Fe<sub>3</sub>O<sub>4</sub>@SiO<sub>2</sub>@KCC-1** (a) and (b).

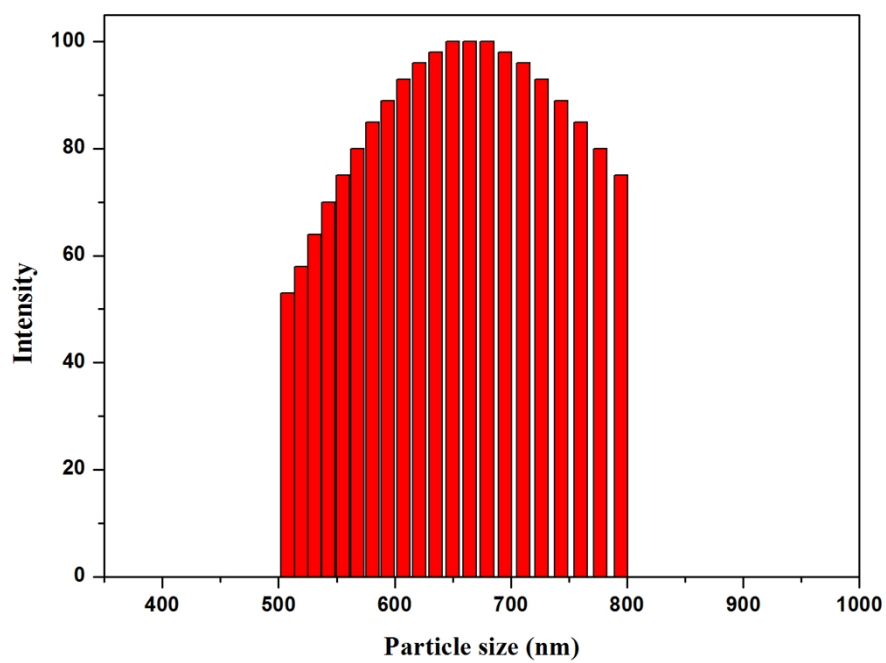


**Fig. S8** The particle size histogram from DLS of AQ- $\text{Fe}_3\text{O}_4@\text{SiO}_2@\text{KCC-1}$ .

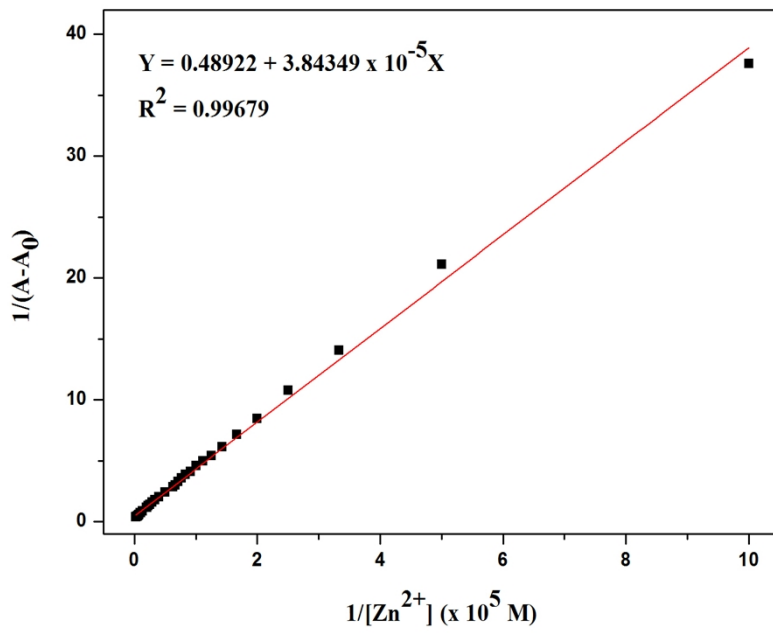


**Fig.S9** Benesi-Hildebrand plot (absorbance at 217 nm) of **AQ-Fe<sub>3</sub>O<sub>4</sub>@SiO<sub>2</sub>@KCC-1** assuming 1:1 stoichiometry between **AQ-Fe<sub>3</sub>O<sub>4</sub>@SiO<sub>2</sub>@KCC-1** and Zn<sup>2+</sup>.

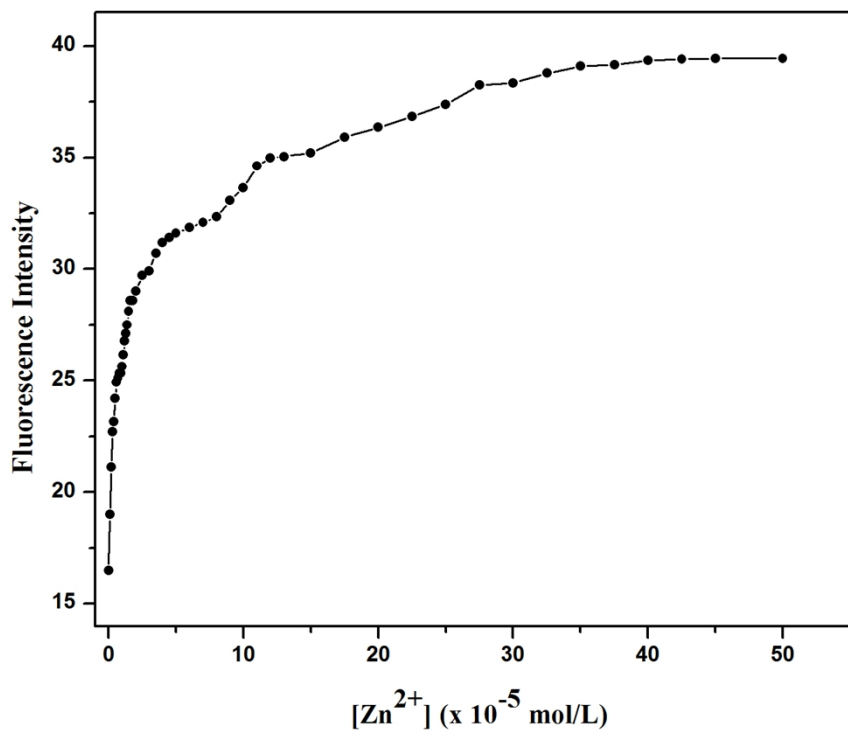


**Fig. S10** Fluorescence intensity at 509 nm of **AQ-Fe<sub>3</sub>O<sub>4</sub>@SiO<sub>2</sub>@KCC-1** (0.1 mg/mL) in Tris-HCl solution (10 mM, pH = 7.20) as a function of Zn<sup>2+</sup> concentration (0-5.0 x 10<sup>-4</sup> M). Excitation at 360 nm.

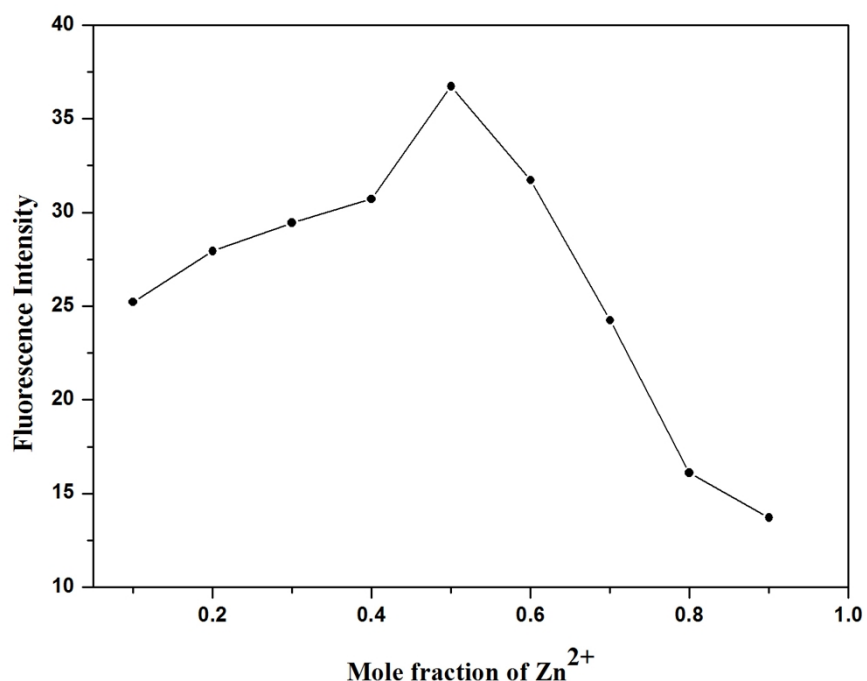


**Fig. S11** Job's plot for determining the stoichiometry of  $\text{AQ-Fe}_3\text{O}_4@\text{SiO}_2@\text{KCC-1}$  and  $\text{Zn}^{2+}$  ions. (The total concentration of  $\text{AQ-Fe}_3\text{O}_4@\text{SiO}_2@\text{KCC-1}$  and  $\text{Zn}^{2+}$  ions was  $4 \times 10^{-5} \text{ M}$ )  $\lambda_{\text{ex}} = 360 \text{ nm}$  and  $\lambda_{\text{em}} = 509 \text{ nm}$ .

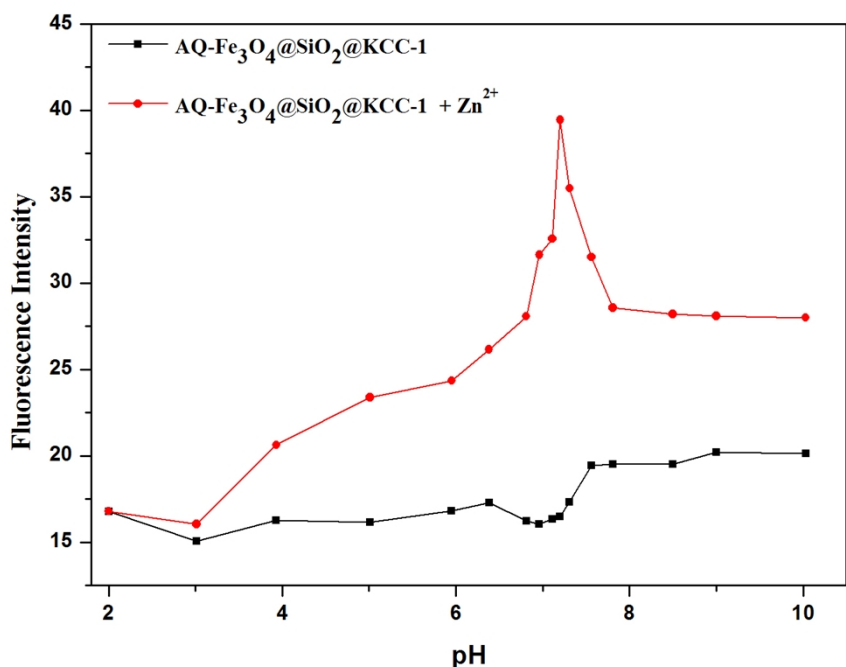


**Fig. S12** Variation of fluorescence intensity at 509 nm of **AQ-Fe<sub>3</sub>O<sub>4</sub>@SiO<sub>2</sub>@KCC-1** (0.1 mg/mL) in Tris-HCl solution (10 mM, pH = 7.20) with and without  $3.1 \times 10^{-5}$  M Zn<sup>2+</sup> as a function of pH. Excitation at 360 nm.

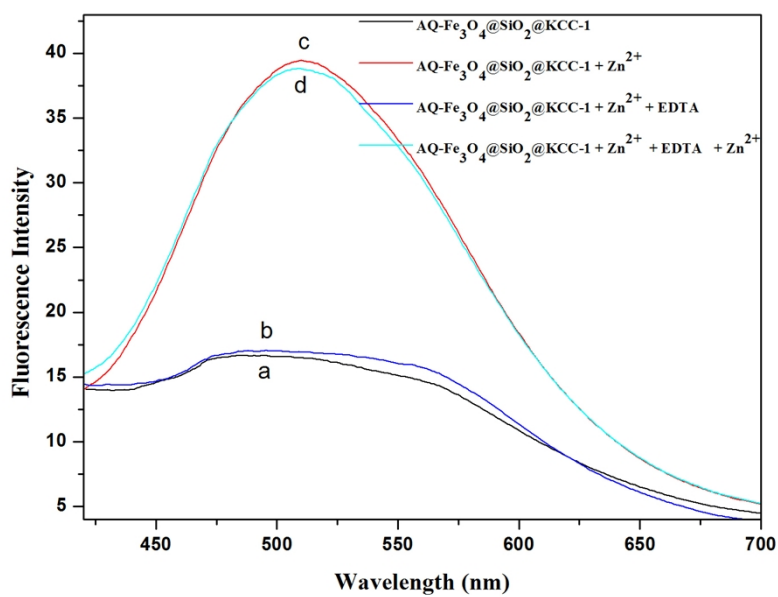


**Fig. S13.** Fluorescence spectra of **AQ-Fe<sub>3</sub>O<sub>4</sub>@SiO<sub>2</sub>@KCC-1** (0.1 mg/mL) in Tris-HCl solution (10 mM, pH = 7.20) a) without, and b) with Zn<sup>2+</sup> ( $5.0 \times 10^{-4}$  M). c) treatment with EDTA ( $5.0 \times 10^{-4}$  M), d) again treatment with Zn<sup>2+</sup> ( $5.0 \times 10^{-4}$  M) in Tris-HCl solution (10 mM, pH = 7.20). Excitation at 360 nm.

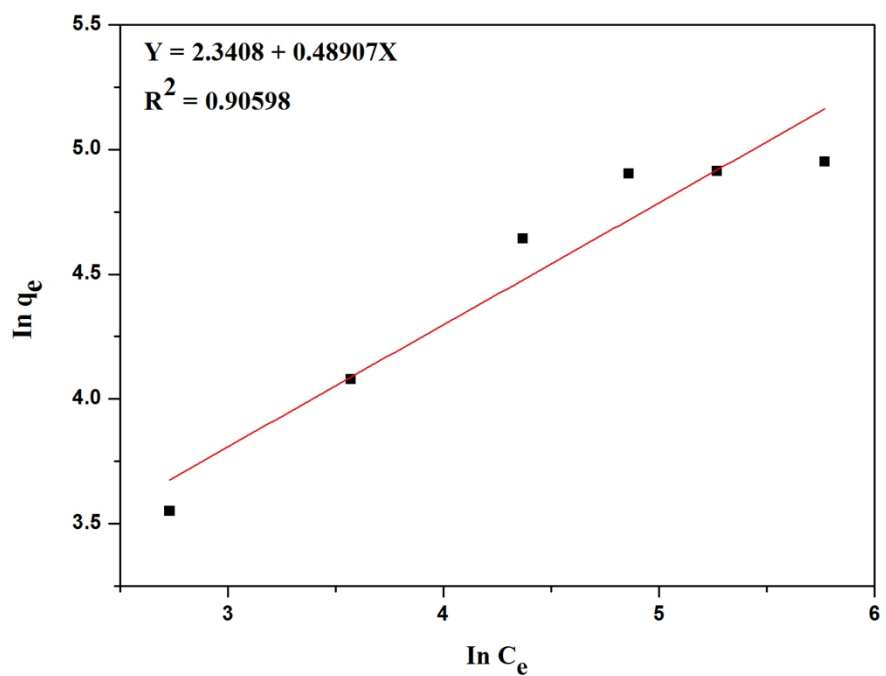


**Fig. S14** Freundlich adsorption isotherm plots for  $Zn^{2+}$  adsorption onto **AQ-Fe<sub>3</sub>O<sub>4</sub>@SiO<sub>2</sub>@KCC-1**.

**Table S1.** Structural properties of  $\text{Fe}_3\text{O}_4@\text{SiO}_2@\text{KCC-1}$  and **AQ-Fe<sub>3</sub>O<sub>4</sub>@SiO<sub>2</sub>@KCC-1**

Samples	$S_{\text{BET}}$ ( $\text{m}^2/\text{g}$ ) <sup>a</sup>	$D_{\text{BJH}}$ (nm) <sup>b</sup>	$V_t$ ( $\text{cm}^3/\text{g}$ ) <sup>c</sup>
$\text{Fe}_3\text{O}_4@\text{SiO}_2@\text{KCC-1}$	213.07	7.94	0.41
<b>AQ-Fe<sub>3</sub>O<sub>4</sub>@SiO<sub>2</sub>@KCC-1</b>	78.76	7.20	0.15

<sup>a</sup> $S_{\text{BET}}$  : BET surface area calculated from data at  $P/P_0 = 0.06-0.29$ . <sup>b</sup> $D_{\text{BJH}}$  : the maximum of the Barret-Joyner-Hellenda (BJH) pore size distribution calculated from the desorption branch of the nitrogen isotherm. <sup>c</sup> $V_t$  : total pore volume calculated at  $P/P_0$  at 0.99.

**Table S2.** Elementary analysis of **AQ-Fe<sub>3</sub>O<sub>4</sub>@SiO<sub>2</sub>@KCC-1**

N (%)	C (%)	H (%)
1.73	8.77	1.032

**Table S3.** The parameters of Langmuir and Freundlich isotherms for Zn<sup>2+</sup> adsorption onto **AQ-Fe<sub>3</sub>O<sub>4</sub>@SiO<sub>2</sub>@KCC-1**.

Adsorption isotherm	parameter	<b>AQ-Fe<sub>3</sub>O<sub>4</sub>@SiO<sub>2</sub>@KCC-1</b>	
		Value of parameter	R <sup>2</sup>
Langmuir	K <sub>L</sub> (L mg <sup>-1</sup> )	0.02896	0.96566
	q <sub>m</sub> (mg g <sup>-1</sup> )	157.2327	
Freundlich	K <sub>F</sub> (L g <sup>-1</sup> )	10.39	0.90598
	n	2.04	